Title

Site-Controlled Plasmon-Assisted Single Photon Emission in Locally Strained Few-Layer Hexagonal Boron Nitride

Authors

Sakib, Mashnoon Alam
Triplett, Brandon
Hussain, Naveed
et al.

Publication Date

2024

DOI

10.1364/cleo_fs.2024.fm2f.5

Site-Controlled Plasmon-Assisted Single Photon Emission in Locally Strained Few-Layer Hexagonal Boron Nitride

Mashnoon Alam Sakib[1], Brandon Triplett[2,3], Naveed Hussain[1], Alexander Senichev[2,3], Xiaohui Xu[2,3], Melika Momenzadeh[1] , Alexandra Boltasseva[2,3], Vladimir M. Shalaev[2,3], and Maxim R. Shcherbakov[1,4,5*]

[1]Department of Electrical Engineering and Computer Science, University of California, Irvine, CA 92697, USA
[2]School of Electrical and Computer Engineering, Birck Nanotechnology Center and Purdue Quantum Science and Engineering Institute, Purdue University, West Lafayette, IN 47907, USA
[3]Quantum Science Center (QSC), a National Quantum Information Science Research Center of the U.S. Department of Energy (DOE), Oak Ridge, TN 37931, USA
[4] Department of Materials Science and Engineering, University of California, Irvine, CA 92697, USA
[5]Beckman Laser Institute and Medical Clinic, University of California, Irvine, CA 92612, USA

Abstract: We report on the site-controlled Purcell-enhanced quantum emitters in hexagonal boron nitride by strain-induced activation in gold-coated silicon nanoposts. The room temperature emitters show a second-order autocorrelation function value at zero time delay $g^{(2)}(0)$ of down to 0.29, lifetimes shortened to 0.5 ns, and single photon emitter yield of 28%.

1. Introduction

Single photon emitters (SPEs) hosted in hexagonal boron nitride (hBN) have emerged as a promising platform for next-generation quantum photonic technologies including quantum communication, optical quantum computing, and quantum sensing[1,2]. hBN, a layered van der Waals (vdW) material with a wide indirect bandgap of ~6eV, is known to host a variety of SPEs that operate a room temperature, exhibiting zero-phonon line energies ranging from ~1.5 to 2.2 eV. The realization of scalable quantum photonic devices often calls for deterministic positioning of bright and indistinguishable SPEs. While recent progress has been made in generating such SPEs in hBN, challenges such as low creation yield, quantum efficiency, and compromised coherence remain a significant motivation for research[3,4].

In this work, we deterministically position bright SPEs in hBN by the use of tall gold-coated silicon posts, which we refer to as a plasmonic nanopillar (PNP) antenna architecture. By transferring hBN on arrays of PNPs, we induce localized nanoscale strain altering the local electronic band structure to deterministically activate SPEs in the visible spectra range. The PNP facilitates coupling between the strain-induced SPEs and the surface plasmons at the tips of the plasmonic nanopillars, resulting in shortened lifetimes and significantly enhanced photoluminescence of these SPEs. The subwavelength radiative processes at the PNP sites exhibit an SPE yield of approximately 28%, single photon antibunching behavior with a second-order autocorrelation function value at zero time delay $g^{(2)}(0)$ value as low as 0.29, and lifetimes down to 470 ps, a five-fold reduction compared to emission from non-plasmonic arrays.

2. Results and discussion

Figure 1(a) shows a schematic of the PNP architecture. To fabricate this structure, electron beam lithography, and reactive ion etching are used to create silicon pillars with heights of 250 nm and radii of 90 nm, arranged into an array with a pitch of 5 μm. A 30 nm layer of gold and a 5 nm alumina spacer layer are deposited onto the silicon nanopillar array through e-beam evaporation and atomic layer deposition, respectively. We then wet-transfer multilayer hBN with ~12 nm thickness onto the array of pillars. Figure 1(b) shows a scanning electron microscope (SEM) image of a PNP with hBN draped over it in a tent-pole-like manner. We performed photoluminescence (PL) mapping of the device with a 532 nm excitation laser using a homebuilt confocal microscope setup as shown in Fig. 1(c). This integrated PL map reveals bright localized emissions associated with strain-activated SPEs originating from the top of the PNPs. The contrast in the PL map among the on-PNP and off-PNP locations demonstrates the nature of this site-controlled SPE generation. In Fig. 1(d-e), the PL spectra from 2 different PNPs (P1 & P2) display the sharp and bright emission lines associated with these two candidate SPEs. These room-temperature PL spectra display narrowband bright emissions with FWHMs of 27 and 40 meV, centered at 618 and 628 nm, respectively. The different classes of emitters arising in this work can be attributed to the draped hBN having variations in strain from pillar to pillar, which may tune the optical properties of the emitter[2,5]. The insets in Fig. 1(d,e) show the second-order autocorrelation measurements with their $g^{(2)}(0)$ values well below 0.5, confirming their single-photon nature. To measure the SPE yield, second-order autocorrelation measurements are performed across 75 different pillars. The pillars are selected

based on their brightness along the square lattice arrangement of the PNPs. After fitting each autocorrelation histogram with a standard 3-level model, the $g^{(2)}(0)$ values are estimated for each PNP as summarized in Fig. 1(g). Of the 75 emitters, 21 have a fitted $g^{(2)}(0)$ value below 0.5 indicating a yield of ≈28% for each pillar to host an SPE. To measure photon antibunching and the lifetime of the SPEs, we performed second-order autocorrelation measurements and time-resolved PL lifetime measurements. In Fig. 1(h), the fitted autocorrelation histograms clearly show that the presence of the alumina spacer layer significantly improves the photon antibunching behavior and purity in terms of the respective $g^{(2)}(0)$ values and their corresponding FWHMs. The 3-level bi-exponential model fitting estimates that $g^{(2)}(0)_{\text{PNP-A}} \approx 0.29$ reaches well below compared to $g^{(2)}(0)_{\text{PNP}} \approx 0.4$. Moreover, the excited state lifetime (τ) estimates show that $(\tau)_{\text{PNP-A}} \approx 1.8$ ns from $(\tau)_{\text{PNP}} \approx 6.6$ ns, resulting in the reduction by a factor of 3.6. Also, the total lifetimes are retrieved from the bi-exponential fitting of the femtosecond-laser-assisted fluorescence decays and are shown in Fig.1(f). The SPEs on alumina-coated PNPs exhibit an average decrease in lifetime by a factor of 4.6 compared to a factor of 2.1 in PNPs without alumina. This demonstrates that the spacer layer is playing a role in preventing the quenching of the emission and allowing for more efficient sub-wavelength radiative enhancement to decrease the emitter's lifetimes. The lowest recorded lifetime that has been measured is 428 ps, which corresponds to a maximum lifetime reduction factor of up to 5.4. To understand the level configuration of the PNP strained defects, we performed incident-power-dependent second-order autocorrelation measurements on an SPE. Fig. 1(i) shows that as the laser excitation power is increased, sequentially from 190 μW/μm^2 to 360 μW/μm^2, the bunching behavior near $\tau = 0$ also improved. This correlated and linear trend in increased power versus the bunching behavior suggests the presence of a metastable state corresponding to a common three-level configuration for a solid-state emitter.

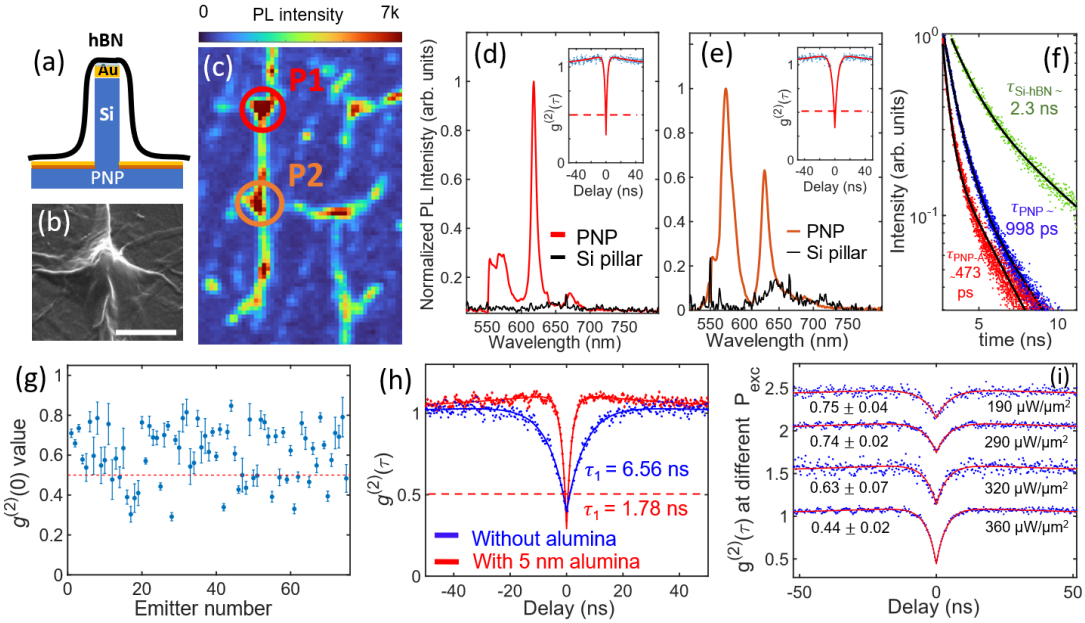

Fig. 1: (a) Schematic of the PNP antenna. (b) Scanning Electron Microscope of the PNP antenna draped with hBN. The scale bar is 2 μm. (c) Confocal PL intensity map of a PNP array portion. Confirmed SPEs are indicated with circles. (d,e) Spectra with the corresponding second-order autocorrelation measurement $g^{(2)}(\tau)$, yielding $g^{(2)}(0)$ of 0.33 and 0.29, corresponding to P1 and P2, respectively. (f) Lifetimes and (g) yield statistics showing the $g^{(2)}(0)$ values for all 75 pillars measured, of which 21 had a fitted $g^{(2)}(0)$ value below 0.5. The error bars show fit uncertainty. (h) Second-order autocorrelation measurements $g^{(2)}(\tau)$ of the emission taken with and without the alumina spacer laser present atop the PNP. With the spacer layer, lifetime shortening is evident by the emission rate enhancement. (i) Power-dependent second-order autocorrelation histograms of a representative emitter.

This work is supported by U.S. Department of Energy (DOE), Office of Science through the Quantum Science Center (QSC), DE-AC05-00R22725 and the Air Force Office of Scientific Research (AFOSR) grant FA9550-22-1-0372.

References

[1] Tran, T., Bray, K., Ford, M. *et al.*, *Nat. Nanotech.* 11, 37-41 (2016)
[2] Li, C., Mendelson, N., Ritika, R. *et al.*, *Nano Lett.*, 21, 3626-3632 (2021)
[3] Tran, T., Kianinia, M., Nguyen, M. *et al.*, *ACS Photonics* 5, 295-300 (2018)
[4] Tran, T., Wang, D., Xu Z. *et al.*, *Nano Lett.* **17**, 2634-2639 (2017)
[5] Proscia, V.N., Shotan, Z., Jayakumar, H. *et al., Optica* **5**, 1128-1134 (2018)